



TMA-Mate: An open-source modular toolkit for constructing tissue microarrays of arbitrary layouts

Nikolaos Pazaitis*, Alexandra Kaiser

Institute of Pathology 'Georg Schmorl', Municipal Hospital Dresden, Campus Friedrichstadt, Friedrichstrasse 41, 01067 Dresden, Germany



ARTICLE INFO

Article history:

Received 14 January 2023
Received in revised form 2 April 2023
Accepted 7 April 2023

Keywords:

Tissue microarray (TMA)
Histopathology
Histology
Biomarkers
3D printing
Open-source hardware

ABSTRACT

Biomedical research and quality control procedures often demand a variety of microscopic analysis of numerous formalin-fixed and paraffin-embedded (FFPE) tissue samples from different individuals of both healthy and diseased regions of interest. Depending on the number of samples to be analyzed, conventional processing of each FFPE block separately can be laborious or impracticable. This effort can be drastically reduced by using tissue microarrays (TMAs). TMAs have a wide range of applications and can be considered as a high-throughput method to process up to hundreds of miniaturized tissue samples simultaneously on a single microscopy slide, in order to reduce labor, costs and sample consumption, and to increase results comparability. Several commercial and self-made solutions to fabricate TMAs with varying degrees of automation are available. However, these solutions may not be suitable for every situation, either due to high costs, high complexity, lack of precision or lack of flexibility, especially when diagnostically oriented pathology institutes or laboratories with constrained resources are considered. This article introduces the TMA-Mate, an open-source 3D printable modular toolkit for constructing high-density TMAs of arbitrary layouts, providing an affordable, lightweight, and accessible procedure to implement TMAs into existing histology processing pipelines. Step-by-step demonstrations for replicating the hardware and constructing TMAs are included.

© 2023 The Authors. Published by Elsevier Ltd. This is an open access article under the CC BY-NC-ND license (<http://creativecommons.org/licenses/by-nc-nd/4.0/>).

Specifications table

Hardware name	TMA-Mate (toolkit for constructing tissue microarrays of arbitrary layouts)
Subject area	<ul style="list-style-type: none"> Medical (Histology/ Histopathology)
Hardware type	<ul style="list-style-type: none"> Biological sample handling and preparation
Closest commercial analog	Tissue microarray mold kits
Open source license	CERN Open Hardware Licence Version 2 - Strongly Reciprocal (CERN-OHL-S-2.0)
Cost of hardware	~ 15 € (first unit), ~ 3–5 € (each subsequent configuration)
Source file repository	https://doi.org/10.17632/76msnn2tz8.1

* Corresponding author.

E-mail address: nikolaos.pazaitis@klinikum-dresden.de (N. Pazaitis).

Hardware in context

Most of the human tissues obtained by surgical resection or autopsy are usually examined and processed macro- and microscopically by pathologists. Diagnostically relevant parts are subsequently preserved and archived for decades as formalin-fixed and paraffin-embedded (FFPE) subsamples. Not only in the context of research projects, but also in quality control routines and education a variety of histological or histotopographically controlled analysis of numerous tissue samples from many individuals, organs and regions of interest of both healthy and diseased tissues are required. The effort involved in processing each FFPE sample separately by applying conventional histology methods can be greatly reduced by using tissue microarrays (first description in [1], refinements in [2,3]), especially when many histologic applications are anticipated. Tissue microarrays (TMAs) can be considered as a high-throughput technique, to process up to hundreds of miniaturized tissue samples simultaneously on a single microscopy slide under identical laboratory conditions, in order to reduce labor, costs, and sample utilization and to increase results comparability (reviewed in [4,5]). Like in conventional histology, TMAs can be subjected to primary and special stainings, enzyme histochemistry [6], conventional [7] and various specialized immunohistochemical (IHC) methods [8,9], in situ hybridizations of RNA [10] and DNA [11], as well as mass spectrometry techniques [12,13], digital analysis [10,14–17] and more. TMAs are powerful and valuable with a wide range of applications in clinical routine diagnostics [5,18] tumor marker research [19–21], drug discovery [10,22], deep-learning [23], biobanking [24,25], quality control [5] and education [26]. TMAs have limitations primarily arising from the small analyzable area covered per specimen but have been proven to generate reliable results compared to standard sized histology sections when carefully designed [11,21,27–29]. In addition, adaptations for assays with other material types such as cytological specimens [30], cultured cell lines [31,32], needle core biopsies (review in [33]) and frozen sections [5,34] have been described.

Multiple manual and instrument-assisted industrial manufactured devices with varying degrees of automation as well as self-made methods and tools capable of producing high density TMAs of more than 1,000 samples per array are available (extensive overview in [35]). Regarding FFPE Material and the standard dot matrix arrangement of samples, most of the proposed procedures follow the principle of extracting relevant regions of interest, in the form of tissue cylinders (tissue cores) from preexisting FFPE blocks (so-called donor blocks) and transferring them in a spatially notated arrangement to an empty paraffin block (so-called recipient block) bearing preformed tissue core pockets. Depending on how many of these processing steps are automated, industrially manufactured solutions can be subdivided into manually operated TMA mold kits (approx. 700–1,300 \$), instrument assisted manually operated devices (approx. 15,000–25,000 \$) to semi and high automated high-throughput machines (from 100,000 \$) with correspondingly increasing acquisition costs.

Published self-made manually performed methods are generally low-cost techniques, differing mainly in the procedure of recipient block fabrication [36–38] (recently reviewed and compared in [37,39]).

Diagnostically focused surgical pathology institutes and laboratories with constrained resources require few selected TMAs, e.g., for participation in collaborative research projects or quality control routines such as on-slide controls and antibody assessments. In such a scenario, investing in a more automated and highly specialized industrially manufactured solution is often not valuable or feasible. Besides high acquisition costs the complexity of these solutions requires user training and creates costly dependencies on the manufacturer regarding service, consumables and replacements. For the laboratories mentioned, the cost-effective and elegant TMA mold kits and self-made methods are much more appropriate.

In this article we introduce the TMA-Mate, a highly accessible open-source fully 3D-printable two-step molding system for creating recipient blocks of arbitrary layouts as well as 3D printable accessories for punching devices, facilitating the fabrication of TMAs with up to 523 tissue cores. Due to a modular concept and a parametrized CAD (computer aided design) model, this toolkit is largely reusable, easily modifiable and allows complete control over TMA design with minimal additional effort for each subsequent desired layout. Recommendations for additional essential materials and basic tooling as well as step by step instructions on how to replicate, operate and customize the TMA-Mate are provided and accompanied with video demonstrations. Illustration of the TMA fabrication process and tips for troubleshooting as well as a validation of the Hardware are included.

Hardware description

The principle of TMA construction with the TMA-Mate is a two-step molding process where a modular 3D printed mold is used to create a silicone counterpart, serving in turn as a mold for casting a paraffin recipient block equipped with tissue core pockets. Depending on the desired tissue core diameter either dermal biopsy punches or slightly modified dispensing needles are used in conjunction with the herein presented accessories (stylet and canula grip) to extract and transfer tissue cores from donor blocks to the casted recipient block (Fig. 1).

The TMA-Mate is a multi-part mold, consisting of a mold chamber and a housing as well as a retaining and a sealing system (Fig. 2). Being the central element of the TMA-Mate, the arrayer (A) is substantial for modularity and designed with functionality, versatility, and economy in mind. Construction of a TMA with an alternate layout requires, at the very least, only the creation of an additional arrayer (A). The array layout can be defined in terms of overall dimensions as well as diameter and arrangement of the tissue cores by adjusting a few parameters in the CAD model of the arrayer (A). Independently of the convenient control via parameters, any arbitrary TMA-layout can be achieved by editing the CAD model of the arrayer (A),

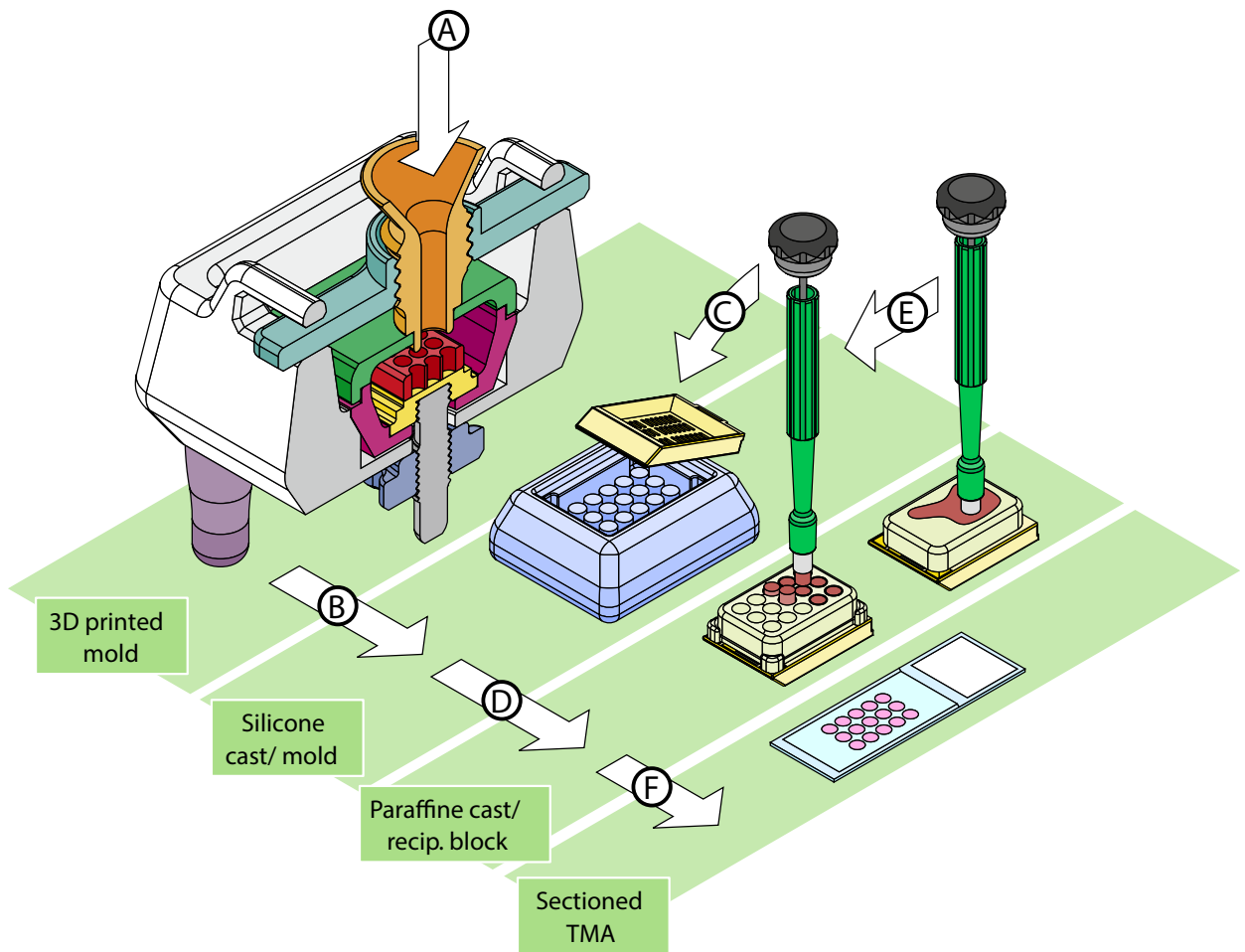


Fig. 1. Principle of TMA generation with the TMA-Mate and the punching devices. A) Following FFF manufacturing of the mold, a silicone cast is formed. B) The silicone cast is demolded and serves in turn as a mold for casting the recipient block by C) pouring paraffin into the silicone mold or submerging the silicone mold into liquid paraffin. A histology cassette is placed into the corresponding recess of the silicone mold. D) The paraffin cast is demolded and serves as a recipient block. E) Tissue cores are punched from donor blocks and transferred to the tissue core pockets of the recipient block. Depending on the tissue core diameter chosen, punching and transferring is done by using either a dermal biopsy punch or the grip and a sharpened dispensing needle in conjunction with the accessories described further below. F) The constructed TMA can be sectioned and processed by applying standard histology procedures.

including TMAs with irregular sized and irregular arranged tissue cores. Optionally, the body (B) and the lid (L) can be customized to label the silicone mold, while the positioner (P) and the arrayer (A) can be modified to label the recipient block.

Although all standard sized histology cassettes should fit with the default settings of the CAD-model, full parametrization allows for adjustments if needed.

In addition to their actual tasks some components have other purposes. The extractor (E) of the holding system and the stylets facilitate the demolding of the silicone mold. Likewise, the rack (R) of the housing prevents accidental contamination of the workplace with liquid silicone during pouring or curing.

Components for the housing (R and S), retaining (N and E) and sealing system (H and F) can be used unchanged for all TMA-layouts while components of the mold chamber and the accessories are mostly interchangeable for different array layouts with equivalent dimensional properties.

Note that all 3D printed components, the silicone molds and the stylets are to a large extent reusable.

In order to maximize the accessibility, we have limited the manufacturing processes to the use of widely available and easy to handle tools and materials, such as an entry-level 3D printer and PLA (polylactic acid) filament. For best results in silicone casting, the introduction of air bubbles must be avoided. For this purpose, it is common to degas the liquid silicone in a vacuum chamber before pouring or to use a pressure tank while curing. To circumvent this specialized tool, the TMA-Mate is designed to cast the silicone mold up-side-down, ensuring collection of unavoidable air bubbles in the functionally unimportant bottom of the silicone cast.

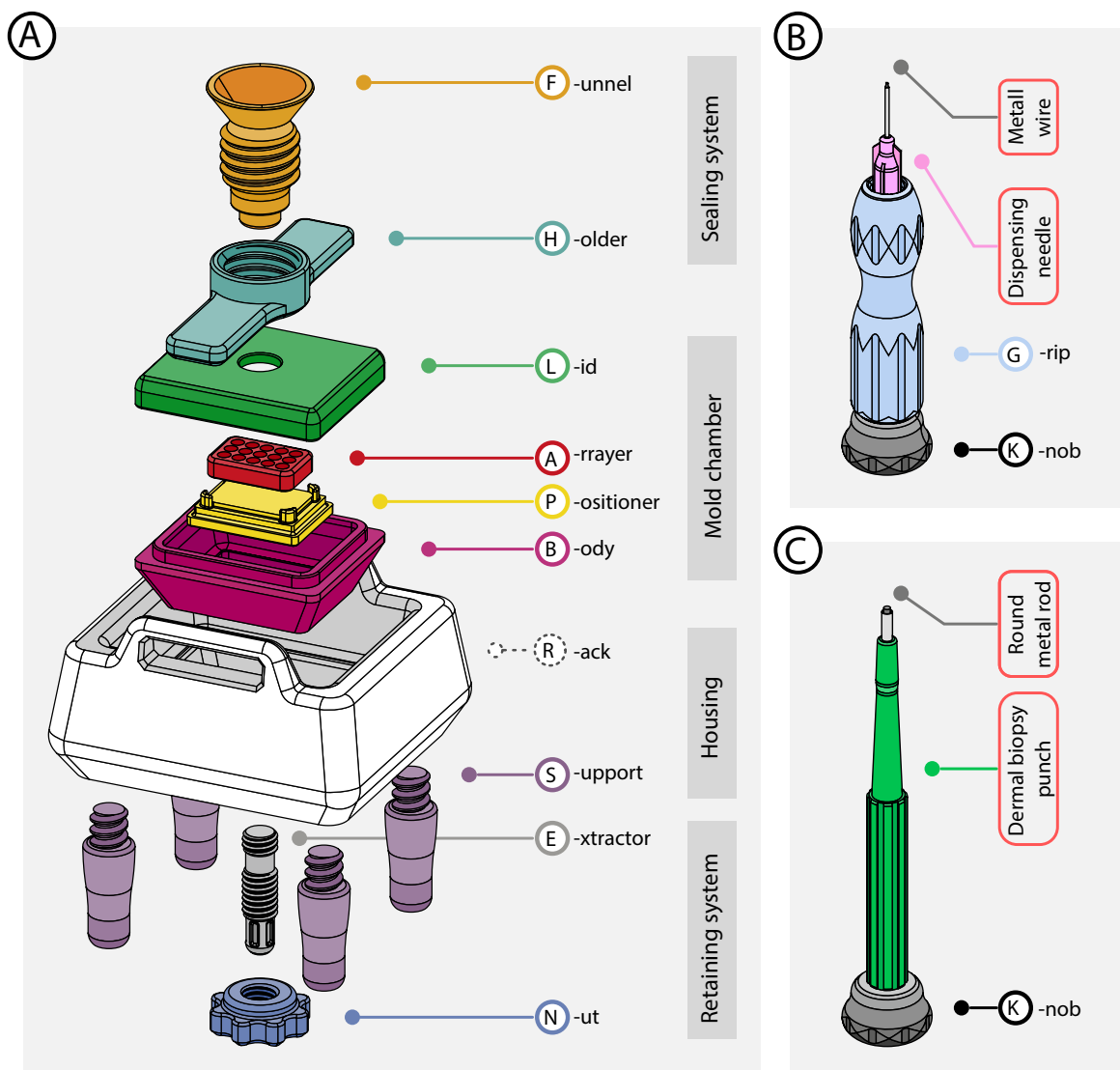


Fig. 2. Overview of the TMA-Mate components and punching devices. A) Exploded view diagram of the TMA-Mate. The 3D printed mold consists of a mold chamber (parts A, B, L and P), a retaining (parts E and N) and sealing (parts F and H) system, and a housing (parts R and S). The arrayer (A) is the central element of the mold, defines the array layout, and is responsible for modularity. Its overall dimensions affect the shape of the positioner. B) Punching devices for tissue core diameters less than 1.0 mm consist of the grip (G) and a sharpened dispensing needle, which can be attached to the Luer-lock located at the tip of the grip (G). A stylet, composed of the knob (K) and a metal wire, is required for ejecting tissue cores from the dispensing needle. 3) For tissue core diameters of 1.0 mm and above, a stylet consisting of the knob (K) and a round metal rod is used in conjunction with dermal biopsy punches.

We prototyped mold designs with down to two and even one-part molds but decide during testing that the here presented multipart design of the 3D printed mold is the most optimal compromise in terms of customizability, ease of modularity, ease of demolding, low failure rate and printing time as well as amount of material and costs needed.

Aim and comparison to existing hardware and methods

The described concept positions our approach between commercially available manually operated TMA mold kits and published self-made methods.

Available TMA mold kits usually include a silicone mold for casting recipient blocks and either dermal biopsy punches or specialized punches for extracting and transferring tissue cores. However, each desired TMA-layout and tissue core diameter requires investing in a new kit. Additionally, these kits restrict sample arrangement and, to our knowledge, are limited to tissue core diameters of 1.0 mm and above. Compared to these products, the TMA-Mate offers more flexibility in terms of

TMA design at a much lower price, as it can accommodate any arbitrary tissue core configuration and diameter (tested for 0.6 to 5.0 mm) by adapting the modular 3D-printed mold followed by an additional silicone cast.

Most published self-made solutions allow great variety in terms of TMA-layout but require cumbersome manual production of the recipient block by extracting paraffin cylinders one by one from a blank solid paraffin block using hollow needles [40,41]. These cost-effective techniques have the disadvantage of being imprecise in the positioning and depth of the tissue core pockets. Compared to these methods, casting the recipient block as proposed here reduces labor and increases accuracy in terms of tissue core pocket positioning, depth and straightness. Some more technically advanced self-made methods increase precision by using a stencil, but still remain quite laborious considering recipient block fabrication [37,42]. Furthermore, effective self-made silicone molds have also been described, but they are hand-made and therefore not precise and only suitable for arrays with few samples and large core diameters [38,43].

The advantage of the TMA-Mate in terms of more precise positioning of the tissue core pockets and the reduced workload also exists compared to even more expensive devices such as the widely used manual tissue arrayer (MTA-1, Beecher Instruments Inc., USA). This manually operated device guides a hollow needle vertically into a solid paraffin block while limiting the depth of the created tissue core pocket. However, each tissue core pocket must be manually punched sequentially, and the recipient block must be repositioned between each punch on a guided hand operated micrometer cross table. Devices like this ensure accurate depth, straightness and squareness to the surface of the tissue core pockets, but not the alignment in x- and y-direction. Additionally, this and all other methods that involve creating tissue core pockets sequentially bear the risk of breaking the recipient block halfway through, potentially requiring the procedure to be restarted.

The TMA-Mate aims to combine the benefits and eliminate the weaknesses of the TMA mold kits and self-made methods and to provide a cost-effective integration of high-density efficiently and accurately constructed TMAs of arbitrary layouts into existing histology processing pipelines for diagnostically focused pathology institutes and laboratories with limited resources. The TMA-Mate

- Implements high throughput histological analysis of up to 523 tissue samples per paraffin block and microscopy slide into existing histology processing pipelines,
- allows arbitrary TMA layouts due to a modular structure,
- is easily adaptable, e.g., to preferred histology cassettes,
- is highly accessible due to open source licensing, and
- can be reproduced with low material and tooling costs.

Design files summary

All files listed below (Table 1), figures and supplementary material were created with open-source software on a PC running Windows 11. The 3D model, the stereolithography files and technical drawings were created with the standard unmodified main distribution of FreeCAD (version 0.20.1, revision number 29410/Git). Vector graphics and Supp. Tab 1 were edited or created with Inkscape (ver. 1.1.2). Slicing was conducted with Ultimaker Cura (ver. 5.1.0). Labels and texts for printed parts, figures and Supp. Tab 1 were set using the free-to-use OpenType Font Jost* (ver. 3.5, created and maintained by Owen Earl).

Contrary to what is shown in the images and videos, labeling of the 3D printed parts is not included in the editable FreeCAD file and STL files. This decision seemed necessary, since FreeCAD currently does not allow font embedding and does not have a comfortable text editing system in the standard distribution. However, this circumstance reduces potential conflicts

Table 1
Design files.

Designator	Design file name	File type	Open source license	Location of the file
A	1. A_Arrayers.zip	Compressed archive file (.zip)	CERN-OHL-S-2.0	https://doi.org/10.17632/76msnn2tz8.1
P	2. P_Positioners.zip	Compressed archive file (.zip)	CERN-OHL-S-2.0	https://doi.org/10.17632/76msnn2tz8.1
B	3. B_Body.stl	Stereolithography file (.stl)	CERN-OHL-S-2.0	https://doi.org/10.17632/76msnn2tz8.1
L	4. L_Lid.stl	Stereolithography file (.stl)	CERN-OHL-S-2.0	https://doi.org/10.17632/76msnn2tz8.1
E	5. E_Extractor.stl	Stereolithography file (.stl)	CERN-OHL-S-2.0	https://doi.org/10.17632/76msnn2tz8.1
N	6. N_Nut.stl	Stereolithography file (.stl)	CERN-OHL-S-2.0	https://doi.org/10.17632/76msnn2tz8.1
H	7. H_Holder.stl	Stereolithography file (.stl)	CERN-OHL-S-2.0	https://doi.org/10.17632/76msnn2tz8.1
F	8. F_Funnel.stl	Stereolithography file (.stl)	CERN-OHL-S-2.0	https://doi.org/10.17632/76msnn2tz8.1
R	9. R_Rack.zip	Compressed archive file (.zip)	CERN-OHL-S-2.0	https://doi.org/10.17632/76msnn2tz8.1
S	10. S_Support.stl	Stereolithography file (.stl)	CERN-OHL-S-2.0	https://doi.org/10.17632/76msnn2tz8.1
G	11. G_Grip.stl	Stereolithography file (.stl)	CERN-OHL-S-2.0	https://doi.org/10.17632/76msnn2tz8.1
K	12. K_Knobs.zip	Compressed archive file (.zip)	CERN-OHL-S-2.0	https://doi.org/10.17632/76msnn2tz8.1
CAD-model	13. TMA_Mate_Model.FCStd	FreeCAD file (FCStd)	CERN-OHL-S-2.0	https://doi.org/10.17632/76msnn2tz8.1

1–12. Stereolithography files (.stl) for each individual part of the TMA-Mate and the accessories as shown and labeled in Fig. 2. Compressed archive files (.zip) contain variants of the indicated 3D printed parts. The Rack (file 9. R_Rack.zip) is the only part that requires print supports and is therefore provided with and without print supports.

13. FreeCAD file with fully assembled parametrized model of the TMA-Mate and the accessories.

with the so-called topology naming problem. Note that the stereolithography files for modular parts cannot be offered in all possible variations and are limited to a reasonable selection.

Bill of materials summary

Production of the TMA-Mate and the punching devices is mostly based on fabrication of 3D printed parts. Note that curing of addition(platinum)-cure silicones is mostly inhibited by UV-Resin. When this type of silicone is used, all 3D printed parts should be manufactured using PLA and FFF (fused filament fabrication).

The specified suppliers in the listing below are not mandatory. All required components, tools and consumables can be purchased from any major online vendor and may be available locally in hardware stores and hobby shops.

The prices shown can vary over time and are depending on location due to different taxation (here 19%) and shipping costs (shipping costs are excluded). If more than one unit is planned, consumables can be more cost-effective if purchased in bulk.

The following bill of materials (Table 2) lists all potentially required materials to manufacture TMAs, regardless of the tissue core diameter. Adjust the corresponding positions according to the desired TMA layout as indicated in Fig. 3.

In addition to the materials listed, the following tools and consumables are necessary:

- Personal protective equipment: protective clothing, safety goggles, disposable gloves, and cut-resistant gloves.
- Manufacturing the TMA-Mate: FFF 3D printer (here unmodified 1st gen. Creality Ender 3)
- Post processing the 3D prints: precision knife (e.g. scalpel or X-Acto) and/ or sandpaper (180 to 240 grit).
- Handling the liquid silicone: precision balance, measuring beaker or disposable cup, disposable stirring spatula or motorized rotary stirrer.
- Post processing the silicone: precision scissors, precision knife and round-tipped tweezers.
- Building the punching devices: side cutter/ pliers, ruler, superglue and sandpaper (320 to 400 grit).
- Pouring the recipient block: histology grade paraffin wax and histology cassettes

Build instructions

Optimal TMA layout depends on the specific experimental question and should be carefully considered in advance. TMA design recommendations can only be briefly mentioned here. For a thorough explanation, we recommend reading the excellent advises in [44].

Not only the number, but also the size of the tissue cores must be taken into account. Although there have been isolated reports of TMAs with even smaller tissue core diameters [45], TMAs with up to 200 samples and tissue core diameters in the range of 0.6 to 5.0 mm appear to be commonly used. While it may seem more convenient and valuable to construct TMAs with the largest possible number of samples, high-density TMAs are not always advantageous. Aside from being significantly more difficult to construct, process and analyze, maximizing the sample count comes at the cost of further minimizing the already small sample size. If for example the focus is on discovering new cellular biomarkers, larger core diameters may be more beneficial, particularly for tissues with known low cellularity or inhomogeneous distributed targets within the cell population of interest. In addition, while high sample density increases the value of the TMA, at the same time it increases the risk of losing an even more valuable preparation accidentally during processing. On the contrary, tissue cores with small diameters conserve the donor block and minimize sample consumption. Furthermore, the small area covered may be compensated by using multiple cores per donor block.

Apart from this considerations arrangement of the tissue cores and utilization of markers for sample identification on the array can facilitate the analysis process.

Table 2
Bill of materials.

Component	Number	Cost per unit [€]	Total cost [€]	Source of materials	Material type
PLA Filament	1 (750 g)	21.69	7.87 (Ø 272 g)	https://www.3djake.de	Polymer (PLA)
Dermal biopsy punch	1 (20 pcs)	45.82	2.29 (1 pcs)	https://www.cis-med.de/	Other
Wire/ round rod	1 (20 cm)	Ø 1.92	Ø 1.00 (Ø 10 cm)	https://www.evek.de	Metal
Two-part addition(platinum)-cure silicone	1 (500 ml)	16.75	2.68 (Ø 80 ml)	https://www.silikonfabrik.de	Polymer (silicone)
Dye (optional)	1 (30 g)	6.75	0.10 (Ø 0.5 g)	https://www.silikonfabrik.de	Other
Dispensing needle	1 (50 pcs)	24.75	0.50 (1 pcs)	https://www.distrelec.de	Other
Σ			Ø 14.07		

The use of dye to color code silicone casts is optional. The grip (G) and dispensing needles are required if tissue core diameters less than 1.0 mm are desired. The dermal biopsy punch is required if tissue core diameters of 1.0 mm and above are chosen. The diameter of the wire/ round rod and the hardness of the silicone depends on the desired tissue core diameter (recommendations in Fig. 3). The chosen silicone should have a so-called pot life, i.e., the period of time in which the silicone still has a viscosity that allows pouring of at least 10–15 min.

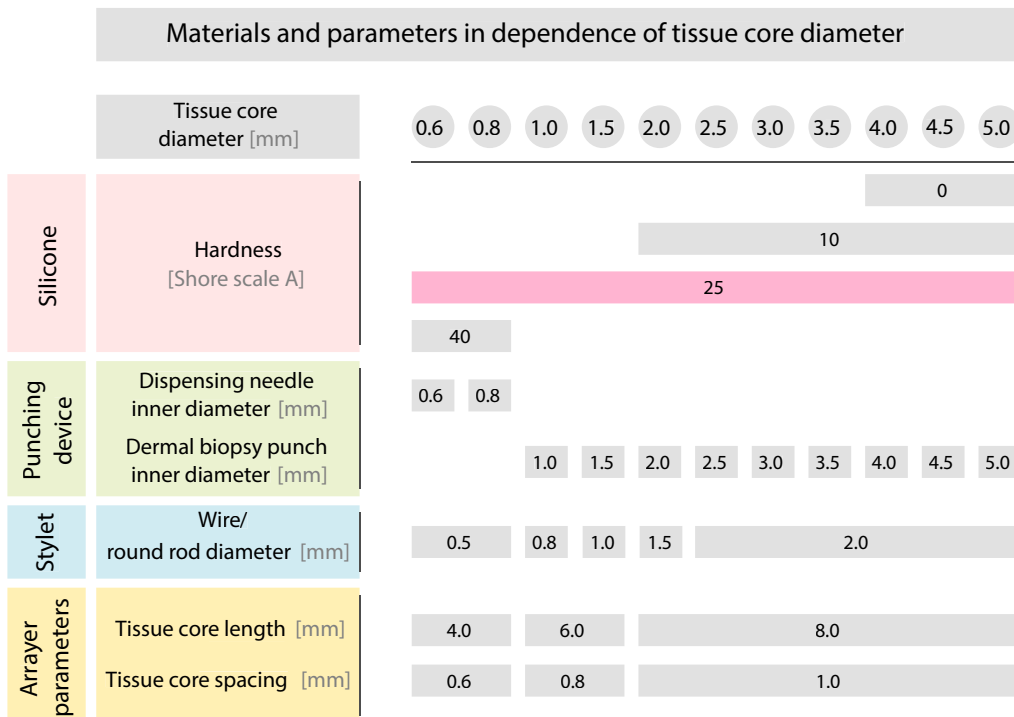


Fig. 3. Materials and parameters in dependence of tissue core diameters. Sufficient hardness of the silicone is necessary to prevent deflection of the pins in the casted mold, particularly for those with small diameters. Two component addition cure silicone with a hardness of 25 on the Shore scale A is recommended as it fits for every tissue core diameter and makes the pins sufficiently mechanically stable and durable. Tissue cores with diameters less than 1.0 mm must be punched with sharpened dispensing needles. Dermal biopsy punches must be used for tissue cores with diameters of 1.0 mm and above. Stylets with round rod diameters of more than 2.0 mm are not recommended as they are heavy and may damage tissue cores during punching and transfer. In addition, although dermal biopsy punches can have an inner diameter of more than 2.0 mm at the tip, they often have a narrow inlet for the stylet.

Regarding all steps outlined in the following sections, it must be noted that the effort, the level of manual skill required, and the probability of failure will increase when tissue core diameters less than 1.0 mm are chosen. For the first attempt, it is recommended to start with a TMA layout that comprises tissue core diameter of 2.0 mm or larger as we consider this to be a good compromise between the difficulty of printing, casting, demolding of the arrayer (A), tissue core transfer and suitability for a wide range of applications.

Safety considerations and disclaimer

The authors of this article hereby deny liability for any material or economic loss as well as damage or injury of health arising in connection with the use or misinterpretation of the information contained in the following sections. Necessary safety precautions depend on the devices, chemical products and tools used in each specific case and can therefore not be listed here for all situations. In all cases: Ensure adequate room ventilation during 3D printing. Pay attention and consider the potential for injury from moving and heated machine elements, especially when using non-enclosed 3D printers. Consult your 3D printer manufacturer’s instruction manual for further safety considerations during FFF fabrication.

Adjusting the CAD model to the experiment requirements

The CAD model was created with the standard unmodified main distribution of FreeCAD (Version 0.20.1, revision number 29410/Git) and is entirely parametrized. However, only three main groups of parameters, need to be adjusted for successful replication and adaptation to the desired TMA Layout. These parameters (i) control the tolerances between interlocking parts, (ii) determine the size of the preferred histology cassettes and (iii) define TMA layout (the latter two are illustrated in Fig. 4, parameters are exposed in the spreadsheet “parameters” in the “TMA_Mate_Model.FCStd” file and can be adjusted as demonstrated in Supp. Vid. 1, also refer to the parameter recommendations in Fig. 3.).

The arrayer (A) is the central element of the TMA-Mate and requires special attention as it defines the TMA-layout and is substantial for modularity. It is small and interchangeable to establish a material and time saving modular system. The simple shape was chosen to allow manufacturing with more precise machining processes such as CNC(computer numerical

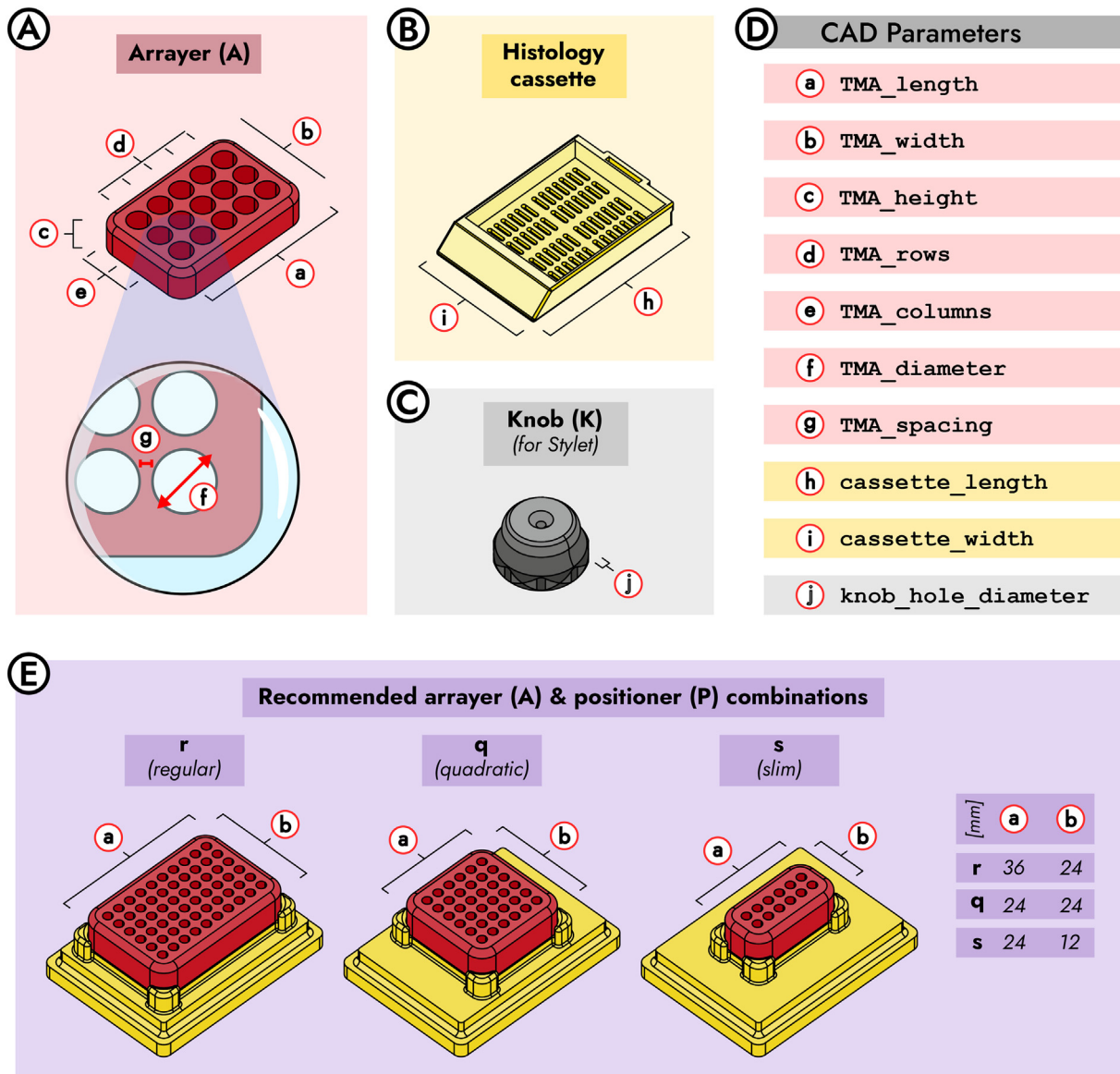


Fig. 4. Essential adjustable parameters of the CAD model and recommended combinations of the arrayer and positioner. A) The arrayer defines the TMA layout and can be adjusted using parameters 'a' to 'g' to accommodate regularly configured TMAs, i.e., TMAs with equally sized samples, regularly arranged in rows and columns in a dot matrix pattern. Recommended values of the parameters 'f' and 'g' with respect to tissue core diameters are provided in Fig. 3. B) With the default CAD settings, the recess in the silicone mold can accommodate histology cassettes with a length of 40–42 mm and a width of 28–30 mm. If other sizes are preferred, it is possible to adjust the model with the parameters 'i' and 'h' accordingly. C) Note that the model of the knob (parameter 'j') adapts to the tissue core diameter (parameter 'f') and the positioner adapts to the dimensions of the arrayer (parameters 'a' and 'b') automatically. D) The listed parameters are exposed and editable in the spreadsheet 'parameters' in the 'TMA_Mate_Model.FCStd' file. E) The depicted outer TMA dimensions and their corresponding values for parameters 'a' and 'b' are recommended. To minimize the number of positioners required, it is advisable to use a limited number of different TMA sizes.

control)-milling from more robust materials such as aluminum. The continuity of the tissue core pockets through the whole part is necessary for preventing air trapping during the casting process and for facilitating the demolding process.

The arrayer (A) can only be parametrically adjusted for regularly configured TMAs. Meaning TMAs consisting of equally sized samples, regularly arranged in rows and columns in a dot matrix pattern (Fig. 4 and Supp. Vid. 1). Irrespective of this, any arbitrary configuration can be created, including arrays with irregular distributed or unequally sized samples by editing the CAD-Model of the arrayer (A). Note that the model of the positioner (P) and the knob (K) of the stylet adapt accordingly depending on the selected dimensions of the arrayer (A) and the chosen tissue core diameter automatically. It is recommended to keep the dimensions of the arrayers (A) consistent in order to minimize the number of positioners (P) needed (recommendations in Fig. 4). We consider the following three sizes to be sufficient for most scenarios:

- r – regular: Maximize the number of samples for the given space on the recipient block
- q – quadratic: Allows the placement of two TMA-sections on a single slide. This situation can be used to increase the number of specimens per slide by combining sections from two different TMAs, or to minimize the chance of tissue loss during further processing by combining two consecutive sections of the same TMA.
- s – slim: Suitable for on-slide-controls in diagnostic routine and antibody assessment.

3D print and slicer settings

Although some parts of the mold would benefit from the higher accuracy of SLA printing, and there are ways to overcome the mentioned inhibition (explanations in section 4), simplicity and wider availability led us to choose FFF manufacturing. Avoid SLA printing when using addition-cure silicone. The TMA-Mate and the accessories are optimized for FFF printing. In case of a mismatch between interlocking parts, only the smaller partner needs to be reprinted as the model always applies the tolerances to the inner part. This strategy helps to reduce material consumption and printing time. To establish reasonable tolerance values, it is recommended to print the arrayer (A) and the positioner (P) first.

The maximum overhang angle of all parts, including threads, is limited to 45°. So-called elephant feet are prevented by compensating beveled edges on the bottom of each part. Except for the rack (R) no supports are needed. For convenience, the model of the rack (R) is provided with and without prebuild minimal supports. The funnel (F) and the lid (L) must be printed upside down. Depending on the bed adhesion capabilities of the used printer it is recommended to print the arrayer (A) with a brim to ensure a flat bottom. Likewise, the positioner (P) should be printed with ironing of the top layer enabled to ensure as much coplanarity as possible with the arrayer (A). Since the area covered by the first layer of the funnel (F) is small, printing with a brim is recommended to improve build plate adhesion. The parts with fine threads (E, G, N and P) and the arrayers (A) should be printed with a nozzle diameter of no more than 0.2 mm and a layer height of 0.12 mm or less. All other parts can be printed with a nozzle diameter of 0.4 mm and a layer height of 0.2 mm. More detailed recommended print and slicer settings for each individual part are summarized in the [Supp. Tab. 1](#).

Post processing the printed parts

Step-by-step instructions for postprocessing the 3D printed parts are shown in [Supp. Fig. 1](#). Post processing is critical for the arrayer (A), in particular for smaller tissue core diameters.

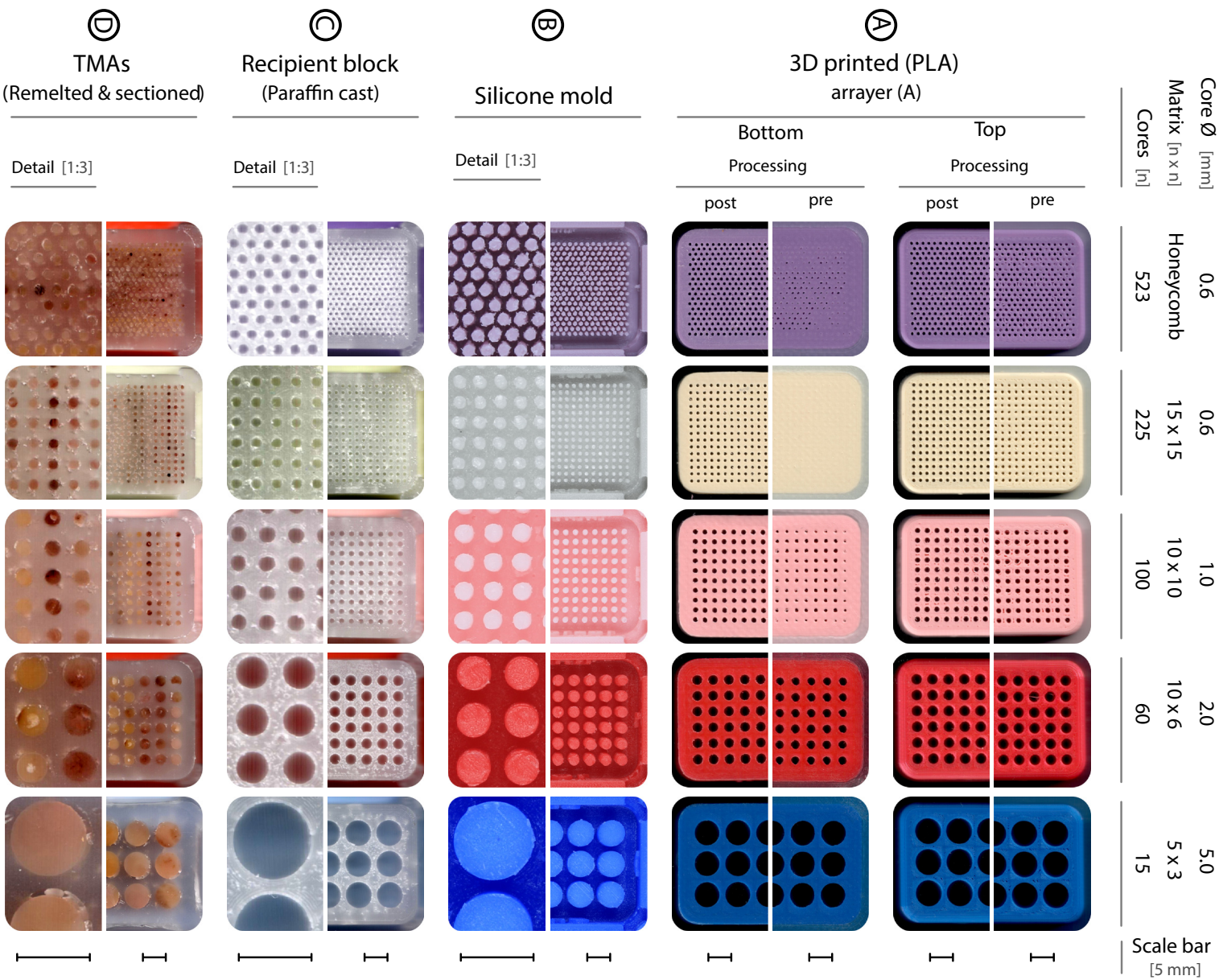
- Remove the supports from the rack (R) and if any used, roughly remove the brim from 3D printed parts ([Supp. Fig. 1A](#)). To properly fit the arrayer (A) into the positioner (P), it may be necessary to use a precision knife and/or sandpaper to completely remove the brim ([Supp. Fig. 1B](#)).
- Depending on the accuracy of the first layer printed, the bottom part of the tissue core pockets on the arrayer (A) may have a slightly smaller diameter or be entirely occluded for diameters below 2.0 mm. To ensure continuity and uniformity of the tissue core pockets, it is required to use a hand drill with the exact anticipated tissue core diameter to remove any excess material by drilling through each pocket ([Supp. Fig. 1C](#)).
- Since the contact surface of the arrayer (A) and the positioner (P) should be coplanar, it is advisable to sand the underside of the arrayer (A) with sandpaper (240 grit or higher, [Supp. Fig. 1D](#)).

Results of postprocessing is shown for the top and bottom surfaces of various arrayers (A) in [Fig. 5A](#).

Preparing the dispensing needle

Although most dispensing needles can be used without, sharpening the tips with sandpaper (320 to 400 grit) before punching reduces potential damage to the donor blocks (step-by-step instructions in [Supp. Fig. 2](#)).

Fig. 5. Stages in constructing regular and alternatively patterned TMAs with the TMA-Mate and the punch devices. TMAs with tissue core diameters ranging from 0.6 to 5.0 mm and sample counts from 15 to 523 are feasible. A) Top and bottom surfaces of various arrayers are shown before and after postprocessing. It is observable, that the lower openings of the tissue core pockets for diameters less than 2.0 mm are partially or completely occluded, which complicates postprocessing. B) Generated silicone molds and C) recipient blocks. Microbubble formation can be observed in recipient blocks with tissue core diameters of 2.0 and 5.0 mm (far right enlargements). This usually occurs if the silicone molds are not properly heated to the temperature of the liquid paraffin prior to casting or if the silicone mold is not adequately cooled on a cooling plate after casting. However, functionality of the recipient blocks is not impaired by the microbubbles in the shown amount. D) Recipient blocks filled with tissue cores transferred from donor blocks after remelting and sectioning procedure. Note that, even when remelting did not fully fuse the tissue cores with diameters of 5.0 mm (far right enlargement), the generated TMA could be sectioned properly with a standard sledge microtome.



Manufacturing the stylet and assembling the punches

After extraction of tissue cores from the donor blocks, the stylet is required to drive the tissue cores out of the hollow needle. The construction of the stylet depends on the desired tissue core diameter (choose wire/ rod diameter according to the listing in Fig. 3). For tissue core diameters of 1.0 mm and above the stylet consists of the knob (K) and a rigid round rod. For diameters below 1.0 mm the grip (G) is required additionally. Any rigid round material can be used for the stylet. While lighter materials such as aluminum or carbon fiber are easier to handle and advantageously offer less resistance to tissue entering the punch during extraction, they are also more difficult to obtain. Here we used brass for wider diameters and stainless-steel wire for diameters less than 1.0 mm. Step-by-step instructions are demonstrated in Supp. Fig. 3 and Supp. Fig. 4.

- For tissue core diameters of 1.0 mm and above: Measure the length of the dermal biopsy punch at hand and add 11.0 mm (10.0 mm knob insertion length plus 1.0 mm front overhang).
- For tissue core diameters less than 1.0 mm: Measure the length of the grip (G) with the dispensing needle attached and add 11.0 mm (Supp. Fig. 3A).
- Cut the round rod or wire to the calculated length with a side cutter or pliers (Supp. Fig. 3B).
- Optionally: Using sandpaper with a grid of 240 to 400 to remove sharp edges on freshly cut round rods or wires will prevent damage to the tissue cores (Supp. Fig. 3C).
- If necessary, drill into the hole of the knob (K) to remove any excess material (Supp. Fig. 3D).
- Apply glue to the opening of the knob (K), insert the wire/rod and let it dry (Supp. Fig. 3E and F).
- The dispensing needle can now be secured to the Luer lock integrated in the tip of the grip (G) and the stylet can be inserted into the dermal biopsy punch or the grip (G, Supp. Fig. 4).

Operation instructions

The following procedures are identical for all TMA layouts, but become significantly more difficult the smaller the tissue core diameter is chosen.

Safety considerations

Safety considerations from section 5 apply. General safety precautions should be followed when handling potentially hazardous substances such as biological material, hot paraffin wax, liquid silicone, formalin and staining reagents. This includes wearing protective clothing such as laboratory gloves, safety goggles and a protective mask. The hazardous potential emanating from addition-cure silicones is product-specific and can be found in the respective safety data sheet. Skin and food-safe variants are available but more expensive and not necessary for this application. Caution is required when handling sharp tools such as biopsy punches, exactor knives, scissors and the microtome, which can cause serious cut or needlestick injuries.

Assembling the mold

A Step-by-step demonstration is given in Supp. Vid. 2. Refer also to the exploded view diagram of the mold in Fig. 2A.

- Screw the extractor (E) into the base of the positioner (P).
- Insert the extractor with the attached positioner (E and P) into the designated hole of the body (B), making sure that the positioner (P) is properly seated in its corresponding pocket of the body (B).
- Insert the entire assembly (E, P, and B) into the designated recess of the rack (R), while allowing the extractor (E) to pass through the opening on the bottom of the rack (R).
- Secure the whole assembly to the rack (R) by screwing the nut (N) onto the extractor (E).
- Screw the supports (S) to the rack (R).

Preparing the silicone according to the manufacturer's instruction

Note that the preparation of the silicone depends on the specific product at hand. Two-part addition-cure silicone, as used herein, typically consists of two liquid components (polymer and catalyst) mixed in a specific ratio (here 1 to 1). Refer to the manufacturer's instructions to identify the mix ratio of the silicone at hand.

Make sure you have all necessary mold parts, tools for weighing and stirring as well as consumables on hand and ready to use as the silicone will begin to cure after the catalyst is added. Note that the curing reaction is temperature dependent. Increasing temperatures greatly reduce cure time. This temperature dependence can be used in two ways: First, production of the molds can be accelerated significantly by increasing the temperature (here approx. 2.5 h at room temperature and 20 min at 50 °C). However, be careful not to deform the mold by exceeding the so-called glass transition temperature of your 3D printing material, which is typically 55–60 °C for PLA. Second, the pot life can be extended by pre-cooling the two com-

ponents before mixing, helping to reduce time pressure while casting. This procedure is demonstrated in [Supp. Vid. 3](#) for the silicone used here.

- Combine the two components to a final volume of 80 ml.
- Optionally: Add dye to color-code different TMA-layouts if desired.
- Stir thoroughly (in our experience 3 min for manual stirring and 2 min for stirring with a rotary tool are sufficient). Try to stir gently, especially on the surface, as stirring is the main source of introducing air bubbles into the mixture.

Pouring the silicone and sealing the mold chamber

This procedure is demonstrated in [Supp. Vid. 4](#) for various tissue core diameters.

- Pour the silicone in a slow and thin flow to a single spot from a height of at least 40 cm, making sure to cover the positioner. This so-called high pour reduces the formation of air bubbles in the final silicone cast.
- Center the desired arrayer (A) on the surface of the liquid silicone and let it sink. Agitate the arrayer (A) with tweezers until it slides into the positioner (P) while applying light pressure. Push the arrayer (A) into position, making sure silicone is leaking from each individual tissue core pocket.
- Fill the mold to the edge of the body (B).
- Place the lid (L) on the corresponding support of the body (B).
- Insert the holder (H) into the appropriate slots of the rack (R).
- Screw the funnel (F) into the holder (H), making sure that the lower part of the funnel neck slides into the corresponding opening of the lid (L).
- Pour the remaining silicone into the funnel (F) using the method described above, up to the middle of the funnel opening.
- Allow the silicone to cure according to the manufacturer's recommendations (here 2–3 h at room temperature).

Demolding and cleaning the silicone cast

This procedure is demonstrated in [Supp. Vid. 5](#) for various tissue core diameters.

- When fully cured, loosen and cut off the conical shaped silicone inside the funnel.
- Unscrew and remove the funnel (F).
- Remove the holder (H).
- Unscrew and remove the nut (N).
- Remove the mold chamber from the rack (R).
- Lift off the lid (L) by levering in the gap between the lid (L) and the body (B) with tweezers.
- Peel off the silicone cast from the sidewalls of the body (B) on all four sides.
- Eject the silicone casting from the body (B) by pushing the extractor (E).
- Carefully detach the positioner (P) from the arrayer (A), possibly by alternately pulling on the extractor (E) and levering in the gap between the extractor (E) and the arrayer (A).
- Cut off the cylindrical shaped silicone formed at the bottom of the mold. Pull or cut off any excess silicone bands formed between interlocking mold parts.
- In most cases a membrane-like silicone film has formed in the gap between the positioner (P) and the arrayer (A), which connects all or part of the silicone pins and must be removed. Depending on how coplanar the positioner (P) and the arrayer (A) fit together, the thickness of the membrane will vary (refer the notes for postprocessing the arrayer and the recommended printing settings in [Supp. Tab 1](#) to ensure that the gap between the critical components is as small as possible). The thicker the membrane and the smaller the diameter of the silicone pins, the more difficult it is to remove the membrane. Thin membranes can be pulled off with tweezers. Membranes on Pins with large diameters can be rubbed off. Thick membranes on pins with small diameters must be trimmed carefully with an exactor knife. In [Supp. Vid. 5](#) different methods for removing membranes of different thicknesses from small and large diameter pins are shown.
- To demold the arrayer (A), two techniques can be used in alternation: (i) lifting movements of the arrayer (A) in all directions with the thumbs inserted under the arrayer (A), and (ii) pressing the pins into their pockets with the stylet until all pins are dislodged from their pockets. Finally remove the arrayer (A).
- Cut off excess silicone bands formed between the pillars of the positioner (P) and the arrayer (A).
- Optional: To extend the lifetime of the silicone mold, consider incubating it at 80 °C for 1 h.

Final state of silicone molds for various tissue core diameters that are sufficient for recipient block casting are shown in [Fig. 5B](#).

Casting the recipient block

This procedure is demonstrated in [Supp. Vid. 6](#) for various tissue core diameters.

- Preheat the created silicone mold for 20 min at 60–80 °C (ideally at the same temperature as the liquid paraffine).

- Submerge the created silicone mold in histological grade liquid paraffin wax and shake it slightly to remove air bubbles. While it is possible to pour paraffin into the silicone mold, it is more prone to air bubble formation. Note that once the silicone mold is flooded with paraffin, the tissue core pins spontaneously straighten and separate from each other.
- Remove the silicone mold vertically from the paraffin bath.
- Subsequently place a histology cassette into the corresponding pocket of the silicone mold while the paraffin is still liquid. If necessary, fill paraffin up to the edge of the histology cassette.
- Place the mold on a cold plate (-10 °C) for 20 to 30 min to speed up the hardening process.
- Once solidified, carefully demold the recipient block.
- The prepared recipient block should be inspected before being filled with tissue cores. If cracks or irregularities such as large air bubbles or fused tissue core pockets are observed, the block must be discarded.

Casted recipient blocks for various tissue core diameters suitable for TMA construction are shown in [Fig. 5C](#).

Extracting and transferring tissue cores from donor to recipient blocks

This procedure is demonstrated in [Supp. Vid. 7](#) for various tissue core diameters.

- Under microscopic control, mark the region of interest on the preexisting H&E (hematoxylin-eosin) stained slide for each given donor block.
- Identify the marked area on the donor block by matching the section on the slide with the donor block tissue.
- Align the tip of the punching device perpendicular to the marked area.
- Retract the slide and punch into the donor block. Note that punching tissue cores with large diameters can damage the donor block, especially when done near the edges.
- Alternately twist the punch 1–2 times in both directions and pull it out of the donor block. The tissue cylinder should now stick in the hollow needle.
- Eject the tissue cylinder into the designated pocket of the recipient block by pushing the stylet. The tissue core should be flush with the surface of the recipient block.
- Repeat these steps for each given donor block.
- Optional: It is recommended to fill the formed hole in the recipient block with an empty paraffin cylinder in order to maintain its integrity and stability, particularly if further tissue cylinders are to be removed from the adjacent area.

Remelting the donor block

This procedure is demonstrated in [Supp. Fig. 5](#). Since the connection between the transferred tissue cores and the recipient block is loose, the TMA cannot be optimally cut with the microtome. To strengthen the connection between the tissue cores and the recipient block the separate paraffin compartments must be homogenized by remelting (discussed in [\[35\]](#)). While the melting temperature of the paraffin used here is 54 to 56 °C, depending on the specific product in use, this temperature can vary. In consequence, it may be necessary to adjust the remelting temperature and time for the paraffin in use.

- Place the TMA face down on a regular microscopy slide and incubate it at 54 °C for 20 min ([Supp. Fig. 5A](#)).
- Place the paraffin block with the slide on a cooling plate (approx. -10 °C), with the slide facing down for 10 min ([Supp. Fig. 5B](#)).
- Standard paraffin block processing methods can now be applied to the TMA.

Remelted and sectioned TMAs with various tissue core diameters are shown in [Fig. 5D](#).

Validation and characterization

To validate and assess the capabilities of the TMA-Mate in terms of feasibility of the described processes, durability of the molds, and suitability of the TMA sections for quality histology processes with respect to different tissue core diameters, we produced both TMAs with regularly arranged tissue cores and one alternatively patterned TMA. To challenge the TMA-Mate, to evaluate its versatility, and to reveal its limitations we aimed to cover TMAs suitable for both scientific applications and commonly used quality control procedures. Small sample sizes are focused as they maximize sample count, are more difficult to construct and process, and complicate the herein proposed procedures significantly.

Quality of TMAs and their sections can be evaluated based on the degree of tissue loss that occurs during TMA construction (core loss) and processing (sample loss). The extend of tissue loss vary depending on the manufacturing method and other factors, such as quality of donor block tissue, annealing quality between tissue cores and the paraffin matrix of the recipient block, and physical intensity of histological processing. However, in our proof of principle, quantification of tissue loss would not be representative due to the selection bias inherent in the choice of optimal donor blocks and regions of interest for tissue core extraction. In actual experiments selection of samples and regions of interest can be greatly constrained, which leads to higher degrees of tissue loss. Therefore, only technically induced tissue loss can be evaluated in the following.

Anonymized redundant tissue from different origins such as lymphatic tissue as well as malign and benign tumorous tissues and adjacent healthy tissues of epithelial and mesenchymal origin were used to represent variability in tissue hardness, density and consistency on the same TMA.

Usability and durability of the 3D printed and silicone molds

To date we have cast and demolded up to 17 silicone molds in one TMA-Mate unit, reusing the same 3D printed parts but swapping the arrayers (A) between casts, with no observable signs of external wear. In addition, we cast up to 13 recipient blocks in one individual silicone mold at paraffin temperatures of 65° to 80° C, preheating the silicone mold for up to 60 min and immersing it in liquid paraffin for up to 15 min. While silicone and paraffin casting and paraffin demolding is easy regardless of tissue core diameter, silicone demolding, especially for small tissue core diameters, requires practice and sure instinct. During our test phase, we found that demolding of the arrayer (A) becomes easier if they have already been used for casting before.

During these repeated procedures we did not notice any impairment of the mold or quality degradation of casted recipient paraffin blocks for tissue core diameters of 1.0 mm and above. Regarding silicone molds with tissue core diameters of 0.6 mm, in one case we lost two core pins during demolding of a silicone cast and one core pin during demolding of a recipient block on a silicone mold that has already been used several times. Presumably due to microbubbles within the thin core pins resulting from suboptimal silicone molding. However, it is also possible that the here used silicone may not be sufficiently tear-resistant for repeated casting of recipient blocks with tissue core diameters of 0.6 mm.

Even though it is technically feasible as demonstrated here, to the best of our knowledge, no TMA mold kits for tissue core diameters less than 1.0 mm are commercially available. According to our own experiences, manufacturers probably cannot guarantee sufficient durability and longevity for these small diameters, thus avoiding the offering of such silicone molds. The use of harder silicone for these delicate silicone core pins could be a potential optimization.

The labeling feature is not essential, but available, has been successfully tested, and can be customized to taste by modifying the CAD-model. Transferring indented and protruding labels from the 3D printed mold parts to its silicone and paraffin counterparts works well and in detail even for small labels. However, placing labels on the body (B) and lid (L) as done here must be chosen carefully. It is advisable to place all necessary labels on a single part, such as the lid (L) to save material and print time when more than one TMA design is desired. We have refrained from making the labeling more convenient as this would further complicate the CAD-model. Alternatively, silicone molds can be labeled manually with a marker or color-coded during casting.

Feasibility of the proposed TMA construction procedure

As accurate matching of tissue cores and their corresponding recipient block pockets is critical for proper TMA sectioning, the usability of the TMA-Mate primarily depends on the ability to produce precise recipient blocks while using simple tools and basic processes such as 3D printed molds and silicone casting without the aid of a vacuum chamber or a pressure tank. In particular, it is important to determine whether error propagation and error multiplication occurring during the two-step molding process make the proposed process unreliable. Casting an accurate recipient block not only depends on an accurate silicon mold, but also on the accuracy of the 3D printed arrayers (A). Our testing demonstrates that the accuracy of the recipient blocks and the self-made punches is suitable for TMA construction of different layouts and commonly used sample sizes. Several stages involved in TMA construction with the TMA-Mate are shown In Fig. 5. Various arrayers (A) and their silicone and paraffin counterparts are shown in their state before and after postprocessing or after tissue core transfer, remelting, and surface trimming, comprising TMAs with up to 523 tissue cores with diameters of 0.6 to 5.0 mm. In addition to TMAs with regular arranged tissue cores in a dot matrix pattern (Fig. 5 second to last column), we constructed a TMA with a honeycomb distribution of tissue cores (described in [46]), which allows for a more efficient utilization of the given space (Fig. 5. left column). Surprisingly, matching of the tissue cores and their pockets is more accurate for smaller diameters. Tissue cores with diameters of 2.0 mm and above tend to be loose and to fall into their pockets (see also Supp. Vid. 7), whereas tissue cores with diameters of 1.0 mm and below are securely retained in their pockets. This may be due to exacerbation of irregularities in tissue cores arising from more challenging manual punching, as precise vertical insertion of punches with larger diameters into donor blocks must be achieved while applying more force. This is observable in the form of residual gaps persisting due to incomplete fusion between tissue cores with large diameters and the paraffin matrix of the recipient block after remelting (Fig. 5D far right enlargement). However, in our hands the proposed overall process is quite forgiving of small inaccuracies in the 3D printed and silicone molds and the manual punching, as following procedure can often compensate for imperfections.

It should be noted that postprocessing of arrayers (A) with numerous tissue cores and small diameters is tedious, as despite fine calibration of the 3D printer, numerous or partially all pockets can be occluded at the bottom of the arrayer (A, Fig. 5A). The effort involved in postprocessing the arrayers (A) may be reduced if a more advanced 3D printer or an even smaller nozzle diameter is used. Despite this, we would like to emphasize that once they have been produced, both the arrayers (A) and the silicone molds can be reused. Therefore, we believe that the effort involved in postprocessing is justified.

Suitability of the constructed TMAs for histology procedures

The functionality of the TMAs was examined in terms of their suitability for proper sectioning using a standard (sledge) microtome and their ability to be processed with routine automated procedures. For processing we choose the most common primary stain H&E, frequently used IHC of both cytoplasmic (cytokeratins, PanCK) and nuclear (proliferation marker Ki-67) antigens, and one brightfield dual color in situ hybridization (BDISH) of DNA of the Her2/neu (surface receptor tyrosine kinase) gene ERBB2 [47] to represent a wide spectrum of physical stress on the sections. Regardless of the number, diameter, and arrangement of their tissue cores, all constructed TMAs were suitable for sectioning, production of consecutive sections and different processing methods with minimal tissue loss. In Fig. 6, gross appearance of sections stained with H&E or processed with IHC and BDISH are shown for both regularly and alternatively patterned TMAs with up to 523 samples per slide. Remarkably tissue loss occurred only in one instance for each TMA with core diameters of either 0.6 or 1.0 mm (Fig. 6A upper row center enlargement and Fig. 6B upper row enlargement). Upon closer inspection of the TMAs, and due to the fact that the particular tissue is lost on each consecutive section of both TMAs, it was found that core loss rather than sample loss occurred on the corresponding positions of both TMAs, most likely due to accidental omission of the pocket on the recipient block during construction. Horizontal bands of light samples in the H&E-stained section in Fig. 6A do not arise due to core or tissue loss, but rather correspond to samples that are predominantly composed of fat tissue, resulting in their pale appearance (Fig. 6A upper row left enlargement). Likewise light staining of samples in the IHC and BDISH sections (Fig. 6A lower two rows) represent tissue with low cellularity or antigen (PanCK) negativity. Note that an additional core appears at the edge of the H&E-stained section (Fig. 6A right enlargement), which could not be found on consecutive sections (Fig. 6A lower two rows), indicating that it originates from contamination while hydrating the section in the floatation bath prior to slide mounting. Partial core loss occurred multiple times in the section undergone harsh BDISH conditions (Fig. 6A lower row right enlargement).

Standard microscopy slides can accommodate two sections for TMAs with quadratic shape (Fig. 6B upper two rows). For the TMA layouts shown, a total of 450 tissue samples can be fitted per histology section for tissue core diameters of 0.6 mm and a total of 200 samples for tissue core diameters of 1.0 mm. This situation can be used to increase the number of specimens per slide by combining sections from two different quadratic TMAs, or to minimize the probability of tissue loss during further processing by combining two consecutive sections of the same TMA (the latter option was applied here). Furthermore, TMAs for quality control procedures (formfactor 'slim') are achievable (Fig. 6C), which can be employed in histology laboratories as daily on-slide controls for special processing procedures such as IHC.

Suitability for microscopy

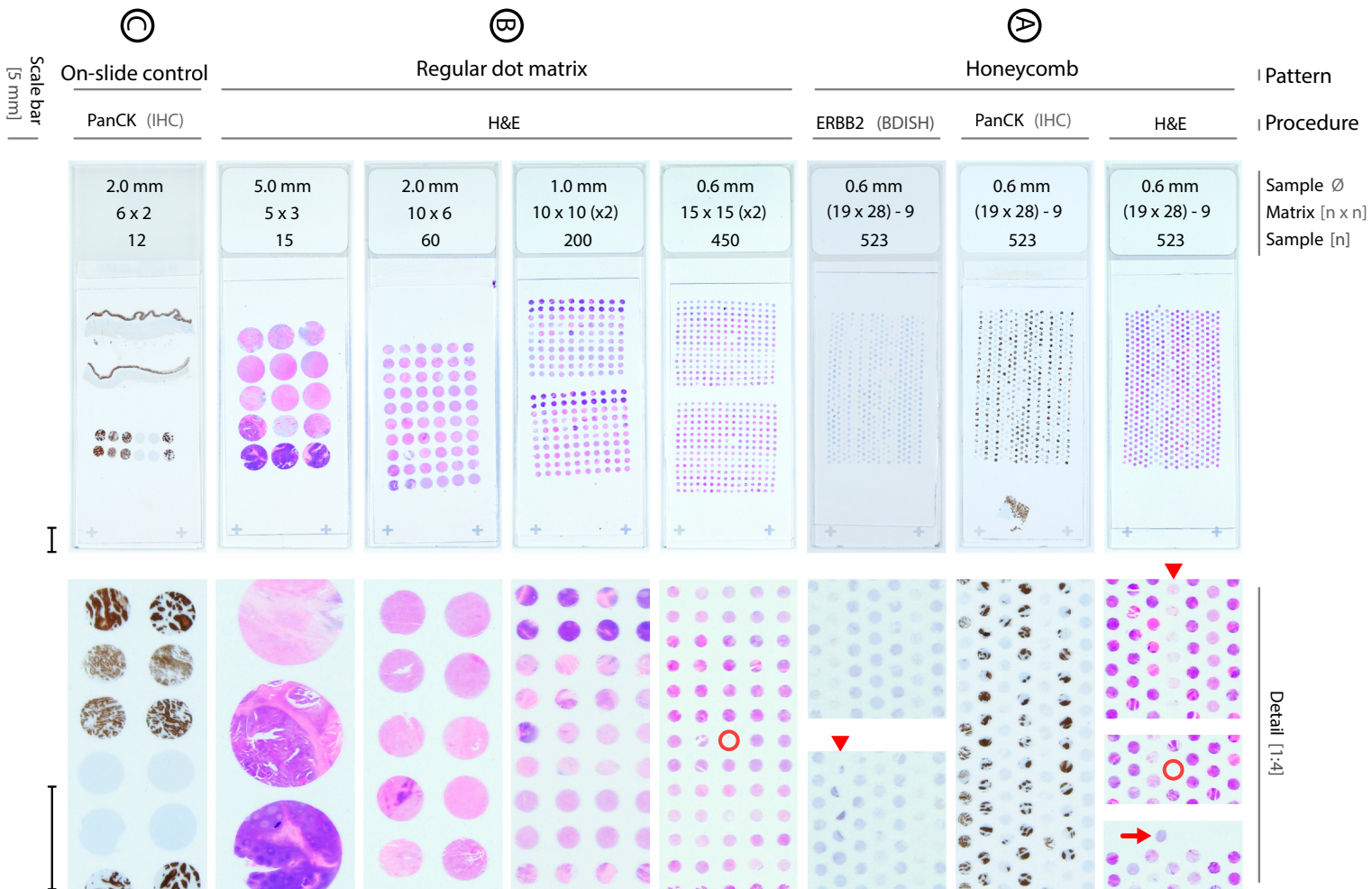
Microscopic examination of TMA sections revealed well preserved histology of all mentioned tissues as shown in Fig. 7 for consecutive Sections of a honeycomb patterned TMA comprising 523 tissue cores with sample diameters of 0.6 mm. Primary staining shows familiar H&E morphology (Fig. 7, upper row). As expected, the adenoma shows the lowest proliferation index (Ki-67) compared to invasive tumors (Fig. 7, third row). Accordingly, cytokeratin positivity can only be observed in epithelial tumors (Fig. 7, second row). Even though BDISH is not intended for all these entities, all samples show nuclei with dual color signals (Fig. 7, lower two rows). The results are convincing and indicate intact morphology and sustained immunoreactivity as well as DNA accessibility for ISH, demonstrating that tissue integrity was preserved during TMA construction and processing.

Capabilities

The TMA-Mate, punch accessories, and proposed procedures enable:

- construction of TMAs with arbitrary layouts,

Fig. 6. Sectioning, H&E staining, IHC, and BDISH are achievable for both regularly and alternatively patterned TMAs constructed with the TMA-Mate and the punching devices. Sections with tissue core diameters ranging from 0.6 to 5.0 mm, comprising up to 523 samples per slide with low tissue loss are depicted. A) The honeycomb pattern enables higher density of tissue cores, thereby maximizing the sample count within the given usable area. Horizontal bands of light samples in the H&E-stained section (upper row) do not arise due to core or tissue loss, but rather correspond to samples that are predominantly composed of fat tissue, resulting in their pale appearance (arrowhead left enlargement). Note that core loss occurred in one instance in the H&E-stained section due to accidental skipping of this position during construction (center enlargement). An additional core appears at the edge of the H&E section (right enlargement), which could not be found on consecutive sections (lower two rows), indicating that it originates from contamination while stretching the section in the floatation bath prior to slide mounting. Partial core loss occurred multiple times in the section undergone harsh ISH conditions (lower row, arrowhead right enlargement). B) Sections of regularly patterned TMAs are shown. Note that standard microscopy slides can accommodate two sections for TMAs with quadratic shape (upper two rows). Note that core loss occurred in one instance for the TMA with core diameters of 0.6 mm. As the core is missing on consecutive sections, most likely core loss rather than sample loss occurred due to accidental skipping of this position during construction (second row enlargement). C) A TMA used for quality control purposes is shown, which can be employed in histology laboratories as on-slide controls for special staining techniques, IHC and ISH on a daily basis. Typically, appropriate tissue is mounted on the edge of the microscope slide (see center row in A) and serves as a positive control. The technique shown here would allow the use of multiple controls.



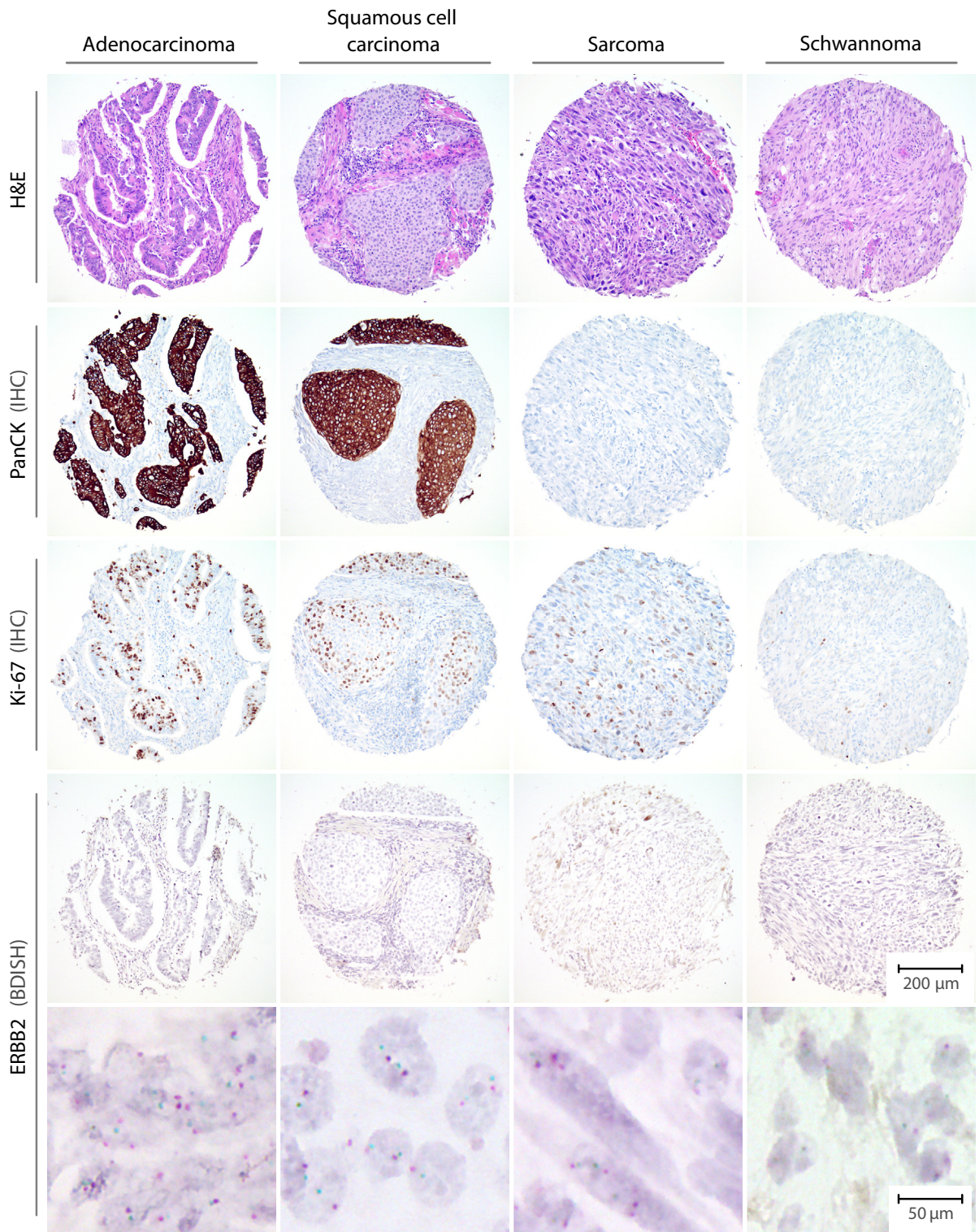


Fig. 7. Consecutive sections of a honeycomb patterned TMA composed of 523 tissue cores with sample diameters of 0.6 mm were processed with H&E staining, IHC, and ISH. Microscopic inspection reveals well preserved morphology of histology sections generated from a TMA produced with the TMA-Mate (upper row). To test cytoplasmic and nuclear immunoreactivity of the tissues, IHC was performed with the frequently assessed antigens Ki-67 (nuclear) and cytokeratin (cytoplasmic). As expected, the schwannoma shows the lowest proliferation index (Ki-67) compared to the carcinomas and the sarcoma (second row). Accordingly, cytokeratin positivity can only be observed in epithelial tumors (third row). Even though BDISH is not intended for all these entities, all samples show nuclei with dual color brightfield signals (fourth row and enlargement in lower row).

- high-throughput histological analysis of up to 523 tissue samples per paraffin block and microscopy slide with minimal tissue loss, while
- ensuring identical processing conditions for each sample,
- sustaining tissue integrity with intact morphology, immunoreactivity, and DNA accessibility for ISH,
- being cost-effective due to the reusability of the punches, 3D-printed parts, and silicone molds, enabled by modular design,
- being time effective as recipient blocks are cast rather than manually constructed, and
- being effortlessly adaptable, e.g., to preferred histology cassettes,
- customizable, e.g., for preferred labeling of silicone molds or recipient blocks,
- and adjustable to the capabilities of the available 3D printer due to parametrization.

Limitations

The limitations of the TMA-Mate mainly concern the construction of TMAs with small tissue core diameters. With further iteration of the model and refined procedures, a large portion of the following disadvantages and limitations may potentially be eliminated.

- Postprocessing of arrayers (A) with many tissue core pockets is laborious. CNC-milling of aluminum arrayers (A) should be considered as an alternative to 3D printing.
- Sample counts of 523 seems to be close to the upper limit for 3D printed arrayers (A). CNC-milling could allow smaller distances between tissue core pockets. The resulting increased density of the samples would result in more usable space for additional tissue cores.
- Demolding of arrayers (A) with small tissue core diameters is tedious. Developing a technique for using (liquid) releasing agents is necessary but challenging as we found interfering capillary effects in the narrow pockets (less than 1.0 mm) of the arrayer (A) during testing.

Ethics statements

According to the competent ethics commission of the Saxonian State Chamber of Medicine, no explicit ethical approval is required for the utilization of anonymized redundant material for demonstrative purposes in this study (reference number: EK-allg-13/22-1). This research was conducted in accordance with the principles stated in the Declaration of Helsinki (amendment 2013) and the (Model) Professional Code for Physicians practicing in Germany (MBO-Ä 1997, amendment 2021).

CRediT authorship contribution statement

Nikolaos Pazaitis: Conceptualization, Methodology, Validation, Investigation, Resources, Writing – original draft, Visualization, Supervision, Project administration. **Alexandra Kaiser:** Validation, Investigation.

Declaration of Competing Interest

The authors declare that they have no known competing financial interests or personal relationships that could have appeared to influence the work reported in this paper.

Acknowledgments

We thank PD Dr. Christiane Jakob for helpful discussions and Dr. Jacqueline Schönlebe for capturing the photomicrographs (Institute of Pathology ‘Georg Schmorl’, Municipal Hospital Dresden-Friedrichstadt, Germany).

Funding

This research did not receive any specific grant from funding agencies in the public, commercial, or not-for-profit sectors.

Appendix A. Supplementary data

Supplementary data to this article can be found online at <https://doi.org/10.1016/j.ohx.2023.e00419>.

References

- [1] H. Battifora, *Methods in laboratory investigation. The multitumor (sausage) tissue block: novel method for immunohistochemical antibody testing*, *Lab. Invest.* 55 (1986).

- [2] Wen-Hui Wan, M.B. Fortuna, P. Furmanski, A rapid and efficient method for testing immunohistochemical reactivity of monoclonal antibodies against multiple tissue samples simultaneously, *J. Immunol. Methods* 103 (1) (1987) 121–129.
- [3] J. Kononen, L. Bubendorf, A. Kallionimi, M. Bärnlund, P. Schraml, S. Leighton, J. Torhorst, M.J. Mihatsch, G. Sauter, O.-P. Kallionimi, Tissue microarrays for high-throughput molecular profiling of tumor specimens, *Nat. Med.* 4 (7) (1998) 844–847.
- [4] R. Simon, G. Sauter, Tissue microarray (TMA) applications: Implications for molecular medicine, *Expert Rev. Mol. Med.* 5 (26) (2003) 1–12.
- [5] M. Mengel, H. Kreipe, R. von Wasielewski, Rapid and large-scale transition of new tumor biomarkers to clinical biopsy material by innovative tissue microarray systems, *Appl. Immunohistochem. Mol. Morphol.* 11 (2003), <https://doi.org/10.1097/00129039-200309000-00010>.
- [6] F. Noack, S. Krüger, C. Thorns, D. Finas, W. Stöcker, K. Diedrich, H.-P. Horny, Application of novel tissue microarrays to investigate expression of tryptase, chymase and KIT protein in placental mast cells, *Arch. Gynecol. Obstet.* 272 (3) (2005) 223–228.
- [7] A. Zimpfer, S. Schonberg, A. Lugli, C. Agostinelli, S.A. Pileri, P. Went, S. Dirnhofer, Construction and validation of a bone marrow tissue microarray, *J. Clin. Pathol.* 60 (1) (2007) 57–61.
- [8] M. Cardano, G.R. Diaferia, M. Falavigna, C.C. Spinelli, F. Sessa, P. DeBlasio, I. Binunno, Cell and tissue microarray technologies for protein and nucleic acid expression profiling, *J. Histochem. Cytochem.* 61 (2) (2013) 116–124.
- [9] W. Huang, K. Henrick, S. Drew, A colorful future for quantitative pathology: validation of vectra technology using chromogenic multiplexed immunohistochemistry and prostate tissue microarrays, *Am. J. Clin. Pathol.* 138 (suppl 2) (2012) A241–A.
- [10] M.K. Singh-Bains, N.F. Mehrabi, A.Y.S. Tan, R.L.M. Faull, M. Dragunow, Preparation, construction and high-throughput automated analysis of human brain tissue microarrays for neurodegenerative disease drug development, *Nat. Protoc.* 16 (4) (2021) 2308–2343.
- [11] E. Sandén, S. Khazaei, H. Tryggvadottir, S. Borgquist, K. Isaksson, K. Jirstrom, H. Jernstrom, Re-evaluation of HER2 status in 606 breast cancers—gene protein assay on tissue microarrays versus routine pathological assessment, *Virchows Arch.* 477 (2) (2020) 317–320.
- [12] R. Casadonte, R. Longuespée, J. Kriegsmann, M. Kriegsmann, MALDI IMS and Cancer Tissue Microarrays, *Adv. Cancer Res.* (2017), <https://doi.org/10.1016/bs.acr.2016.11.007>.
- [13] T.W. Powers, B.A. Neely, Y. Shao, H. Tang, D.A. Troyer, A.S. Mehta, B.B. Haab, R.R. Drake, S.K. Batra, MALDI imaging mass spectrometry profiling of N-glycans in formalin-fixed paraffin embedded clinical tissue blocks and tissue microarrays, *PLoS One* 9 (9) (2014) e106255.
- [14] N.G. Egeland, K. Jonsdottir, K.L. Lauridsen, I. Skaland, C.F. Hjorth, E.G. Gudlaugsson, S. Hamilton-Dutoit, T.L. Lash, D. Cronin-Fenton, E.A.M. Janssen, Digital image analysis of Ki-67 stained tissue microarrays and recurrence in tamoxifen-treated breast cancer patients, *Clin. Epidemiol.* 12 (2020), <https://doi.org/10.2147/CLEP.S248167>.
- [15] G.M. Baker, V.C. Bret-Mounet, T. Wang, M. Veta, H. Zheng, L.C. Collins, A.H. Eliassen, R.M. Tamimi, Y.J. Heng, Immunohistochemistry scoring of breast tumor tissue microarrays: a comparison study across three software applications, *J. Pathol. Inform.* 13 (2022), <https://doi.org/10.1016/j.jpi.2022.100118>.
- [16] M. Abubakar, W.J. Howat, F. Daley, L. Zabaglo, L.-A. McDuffus, F. Blows, P. Coulson, H. Raza Ali, J. Benitez, R. Milne, H. Brenner, C. Stegmaier, A. Mannermaa, J. Chang-Claude, A. Rudolph, P. Sinn, F.J. Couch, R.A.E.M. Tollenaar, P. Devilee, J. Figueroa, M.E. Sherman, J. Lissowska, S. Hewitt, D. Eccles, M.J. Hooning, A. Hollestelle, J. WM Martens, C. HM van Deurzen, kConFab Investigators, M.K. Bolla, Q. Wang, M. Jones, M. Schoemaker, A. Broeks, F.E. van Leeuwen, L. Van't Veer, A.J. Swerdlow, N. Orr, M. Dowsett, D. Easton, M.K. Schmidt, P.D. Pharoah, M. Garcia-Closas, High-throughput automated scoring of Ki67 in breast cancer tissue microarrays from the Breast Cancer Association Consortium, *J. Pathol. Clin. Res.* 2 (3) (2016) 138–153.
- [17] W.J. Howat, F.M. Blows, E. Provenzano, M.N. Brook, L. Morris, P. Gazinska, N. Johnson, L.-A. McDuffus, J. Miller, E.J. Sawyer, S. Pinder, C.H.M. van Deurzen, L. Jones, R. Sironen, D. Visscher, C. Caldas, F. Daley, P. Coulson, A. Broeks, J. Sanders, J. Wesseling, H. Nevanlinna, R. Fagerholm, C. Blomqvist, P. Heikkilä, H.R. Ali, S.-J. Dawson, J. Figueroa, J. Lissowska, L. Brinton, A. Mannermaa, V. Kataja, V.-M. Kosma, A. Cox, I.W. Brock, S.S. Cross, M.W. Reed, F.J. Couch, J.E. Olson, P. Devilee, W.E. Mesker, C.M. Seyaneve, A. Hollestelle, J. Benitez, J.I.A. Perez, P. Menéndez, M.K. Bolla, D.F. Easton, M.K. Schmidt, P.D. Pharoah, M.E. Sherman, M. García-Closas, Performance of automated scoring of ER, PR, HER2, CK5/6 and EGFR in breast cancer tissue microarrays in the Breast Cancer Association Consortium, *J. Pathol. Clin. Res.* 1 (1) (2015) 18–32.
- [18] P. Murugan, D. Shukla, J. Morocho, D. Smith, D. Sciacca, M. Pickard, M. Wahlsten, A. Gunderson, B. Konety, M.A. Khalifa, C. Warlick, Prostate Biopsy Processing: An Innovative Model for Reducing Cost, Decreasing Test Time, and Improving Diagnostic Material, *Am J Clin Pathol* 152 (2019).
- [19] A. Menz, T. Weitbrecht, N. Gorbokov, F. Büscheck, A.M. Luebke, M. Kluth, C. Hube-Magg, A. Hinsch, D. Höflmayer, S. Weidemann, C. Fraune, K. Möller, C. Bernreuther, P. Lebok, T. Clauditz, G. Sauter, R. Uhlig, W. Wilczak, S. Steurer, S. Minner, E. Burandt, R. Krech, D. Dum, T. Krech, A. Marx, R. Simon, Diagnostic and prognostic impact of cytokeratin 18 expression in human tumors: a tissue microarray study on 11,952 tumors, *Mol. Med.* 27 (2021), <https://doi.org/10.1186/s10020-021-00274-7>.
- [20] A. Menz, R. Bauer, M. Kluth, C. Marie von Barga, N. Gorbokov, F. Viehweger, M. Lennartz, C. Völkl, C. Fraune, R. Uhlig, C. Hube-Magg, N. De Wispelaere, S. Minner, G. Sauter, S. Kind, R. Simon, E. Burandt, T. Clauditz, P. Lebok, F. Jacobsen, S. Steurer, W. Wilczak, T. Krech, A.H. Marx, C. Bernreuther, Diagnostic and prognostic impact of cytokeratin 19 expression analysis in human tumors: a tissue microarray study of 13,172 tumors, *Hum. Pathol.* 115 (2021) 19–36.
- [21] E.S. Gruber, G. Oberhuber, D. Pils, T. Stork, K. Sinn, S. Gruber, R. Nica, D. Kolmer, S.D. Turner, M. Schleder, J. Widder, W. Doerr, B. Teleky, L. Kenner, The determination of immunomodulation and its impact on survival of rectal cancer patients depends on the area comprising a tissue microarray, *Cancers (Basel)*. 12 (3) (2020) 563.
- [22] G. Sauter, R. Simon, K. Hillan, Tissue microarrays in drug discovery, *Nat. Rev. Drug Discov.* 2 (12) (2003) 962–972.
- [23] H.G. Nguyen, A. Blank, H.E. Dawson, A. Lugli, I. Zlobec, Classification of colorectal tissue images from high throughput tissue microarrays by ensemble deep learning methods, *Sci. Rep.* 11 (2021), <https://doi.org/10.1038/s41598-021-81352-y>.
- [24] R. Dhir, Prostate cancer biobanking, *Curr. Opin. Urol.* 18 (3) (2008) 309–314.
- [25] S. Lal, A. Li, D. Allen, P.D. Allen, P. Bannion, T. Cartmill, R. Cooke, A. Farnsworth, A. Keogh, C. dos Remedios, Best practice BioBanking of human heart tissue, *Biophys. Rev.* 7 (4) (2015) 399–406.
- [26] H. Wang, H. Wang, W. Zhang, G.N. Fuller, Tissue microarrays: applications in neuropathology research, diagnosis, and education, *Brain Pathol.* 12 (1) (2002) 95–107.
- [27] D. Pilla, F.M. Bosisio, R. Marotta, S. Faggi, P. Forlani, M. Falavigna, I. Binunno, E. Martella, P. De Blasio, S. Borghesi, G. Cattoretti, Tissue microarray design and construction for scientific, industrial and diagnostic use, *J. Pathol. Inform.* 3 (1) (2012) 42.
- [28] U.P. Hacısalıhoğlu, M.A. Dogan, Expression of estrogen and progesterone receptors, HER2 protein and Ki-67 proliferation index in breast carcinoma in both tumor tissue and tissue microarray, *Biotech. Histochem.* 97 (4) (2022) 298–305.
- [29] L.H. Schmidt, S. Biesterfeld, A. Kümmel, A. Faldum, M. Sebastian, C. Taube, R. Buhl, R. Wiewrodt, Tissue microarrays are reliable tools for the clinicopathological characterization of lung cancer tissue, *Anticancer Res.* 29 (2009).
- [30] C.-H. Wen, Y.-C. Su, S.-L. Wang, S.-F. Yang, C.-Y. Chai, Application of the microarray technique to cell blocks, *Acta Cytol.* 51 (1) (2007) 42–46.
- [31] A. Hoos, C. Cordon-Cardo, Tissue microarray profiling of cancer specimens and cell lines: opportunities and limitations, *Lab. Invest.* 81 (10) (2001) 1331–1338.
- [32] A. Waterworth, A. Hanby, V. Speirs, A novel cell array technique for high-throughput, cell-based analysis, *In Vitro Cell. Dev. Biol. Anim.* 41 (7) (2005) 185.
- [33] M. Albanghali, A. Green, E. Rakha, M. Aleskandarany, C. Nolan, I. Ellis, K.-L. Cheung, Construction of tissue microarrays from core needle biopsies – A systematic literature review, *Histopathology* 68 (3) (2016) 323–332.
- [34] M. Schoenberg Fejzo, D.J. Slamon, Frozen tumor tissue microarray technology for analysis of tumor RNA, DNA, and proteins, *Am. J. Pathol.* 159 (5) (2001) 1645–1650.
- [35] U. Vogel, Overview on techniques to construct tissue arrays with special emphasis on tissue microarrays, *Microarrays* 3 (2) (2014) 103–136.
- [36] Y. Shi, D. He, Y. Hou, Q. Hu, C. Xu, Y. Liu, D. Jiang, J. Su, H. Zeng, Y. Tan, An alternative high output tissue microarray technique, *Diagn. Pathol.* 8 (2013) 9, <https://doi.org/10.1186/1746-1596-8-9>.

- [37] Y.J. Chen, C.M. Yang, J.S. Huang, P. Wang, Y.H. Lv, C. Tang, W. Deng, An introduction of an easy-operating and economical technique for tissue microarray preparation, *J. Clin. Pathol.* 73 (2020) 403–407, <https://doi.org/10.1136/jclinpath-2019-206142>.
- [38] S. Gollapudi, K. Singh, C. Small, S. Mukherjee, R.S. Ohgami, Creation of efficient pathology research pipelines for discovery: tissue microarray construction coupled with digital image analysis, *J. Clin. Transl. Pathol.* (2021), <https://doi.org/10.14218/jctp.2021.00012>.
- [39] A.E. Ștefan, D. Gologan, M.O. Leavitt, S. Mușat, I.E. Pleșea, L.G.R. Stan, R.M. Pleșea, M. Militaru, Tissue microarrays – brief history, techniques and clinical future, *Rom. J. Morphol. Embryol.* 61 (4) (2021) 1077–1083.
- [40] K.H. Kim, S.J. Choi, Y.I. Choi, L. Kim, I.S. Park, J.Y. Han, J.M. Kim, Y.C. Chu, In-house manual construction of high-density and high-quality tissue microarrays by using homemade recipient agarose-paraffin blocks, *Korean J. Pathol.* 47 (3) (2013) 238.
- [41] C.H. Choi, K.H. Kim, J.Y. Song, S.J. Choi, L. Kim, I.S. Park, J.Y. Han, J.M. Kim, Y.C. Chu, Construction of high-density tissue microarrays at low cost by using self-made manual microarray kits and recipient paraffin blocks, *Korean J. Pathol.* 46 (2012) 562–568, <https://doi.org/10.4132/KoreanJPathol.2012.46.6.562>.
- [42] W. Zhang, F. Qiu, Q. Jiang, S. Liu, Z. Xiong, Simple method for constructing and repairing tissue microarrays using simple equipment, *Journal of International Medical Research.* 49 (2021), doi: 10.1177/03000605211000156.
- [43] S. Srinath, R. Kendole, P. Gopinath, S. Krishnappa, S. Vishwanath, Economic methods used in fabrication of tissue microarray: a pilot study, *Journal of Oral and Maxillofacial, Pathology* 20 (2016) 86–90, <https://doi.org/10.4103/0973-029X.180948>.
- [44] H. Remotti, Tissue microarrays: construction and use, *Methods Mol. Biol.* 980 (2013) 13–28, https://doi.org/10.1007/978-1-62703-287-2_2.
- [45] U.F. Vogel, The construction of high-density paraffin tissue microarrays with 0.43-mm-diameter paraffin tissue core biopsies is technically feasible, *Virchows Arch.* 453 (1) (2008) 43–46.
- [46] U.F. Vogel, J. Bode, B. Bueltmann, Increasing the efficiency of paraffin tissue microarrays by packing the paraffin tissue core biopsies in a honeycomb pattern, *Appl. Immunohistochem. Mol. Morphol.* 15 (3) (2007) 343–345.
- [47] H. Nitta, B. Hauss-Wegrzyniak, M. Lehrkamp, A.E. Murillo, F. Gaire, M. Farrell, E. Walk, F. Penault-Llorca, M. Kurosumi, M. Dietel, L. Wang, M. Loftus, J. Pettay, R.R. Tubbs, T.M. Grogan, Development of automated brightfield double in Situ hybridization (BDISH) application for HER2 gene and chromosome 17 centromere (CEN 17) for breast carcinomas and an assay performance comparison to manual dual color HER2 fluorescence in Situ hybridization (FISH), *Diagn. Pathol.* 3 (1) (2008) 41.



Nikolaos Pazaitis attended medical school at Martin-Luther-University Halle-Wittenberg (Germany). After graduating and completing an interdisciplinary graduate school (GRK1591 - “Post-transcriptional control of gene expression - mechanisms and role in pathogenesis”), he received his doctorate degree for investigating RNA-binding proteins in cancer while establishing viral gene transfer methods and in vivo non-invasive fluorescence imaging techniques. His interest in tumor biology led to a residency at the Institute of Pathology of the University Hospital Halle (Saale). During this time, he gained experience in Next Generation Sequencing and various imaging technologies such as transmission electron and multispectral microscopy. Reflecting his curiosity for technology and innovation in pathology, he also had the opportunity to develop an online teaching and learning platform for student education using virtual microscopy. Moreover, he contributed to the establishment of a text-to-speech system for histopathology report writing in clinical routine. He is currently continuing his residency training at the Institute of Pathology at the Municipal Hospital Dresden (Germany), solidifying his skills in diagnostic routine. As a digital fabrication enthusiast, he is currently developing affordable alternatives to commercially available microscopy imaging techniques with open-source philosophy in mind.